PCCP

PAPER

View Article Online
View Journal | View Issue

Co-adsorption of water and glycine on Cu{110}†

Marco Sacchi* and Stephen J. Jenkins

Cite this: *Phys. Chem. Chem. Phys.*, 2014, **16**, 6101

Received 3rd December 2013,
Accepted 4th February 2014

DOI: 10.1039/c3cp55094j

www.rsc.org/pccp

In this study, we use density functional theory (DFT) to investigate the surface co-adsorption of glycine with water on Cu{110}. Our results show that, under UHV conditions and for a wide range of temperatures, a pure glycine monolayer is more stable than either mixed gly–water phases or pure water (ice) monolayers, but for a high water pressure half-dissociated water layers can appear on the surface at low and medium temperatures.

1. Introduction

Amino acids are some of the simplest biological molecules, yet they nevertheless manifest the ability to construct an incredibly complex variety of structures in which a delicate balance of intermolecular chemical forces drives the dynamics of self-recognition and assembly. Understanding the mechanism by which chiral structures are naturally synthesized is also extremely relevant to pharmaceutical and biochemical industries, in which enantioselectivity and enantiospecificity are vital factors in producing biologically compatible drugs. In this context, the adsorption of simple, naturally occurring amino acids on single crystal surfaces has become the playground for studying chiral self-assembly at the atomic scale and investigating pathways to enantioselective catalytic synthesis using a bottom-up approach. In particular, in the last two decades, several groups have dedicated a concerted effort to understand the formation of chiral self-assembled supramolecular networks of alanine, glycine and proline on Cu{110},[1–12] Cu{100}[1,5–7,13–24] and Cu{111}[25–28] surfaces. In the past, with few exceptions,[1] the vast majority of the atomistic studies on supramolecular assembly of amino acids on metal surfaces have been conducted under UHV conditions. It is therefore one of the main challenges ahead of the surface-science community to attempt to bridge the gap between experiments conducted under "dry" vacuum conditions (in which the amino acids adsorb in the absence of a solvent and a co-adsorbate) and the more biologically and pharmaceutically relevant "wet" studies. In fact, when water is present in the system, a competition exists between the formation of hydrogen bonds between an amino acid with another and between an amino acid and the water shell immediately surrounding it. The interaction between amino acids and water is also particularly relevant to corrosion protection, since amino acids have recently become a natural and ecologically compatible alternative to traditional amine-based corrosion inhibitors.[29–31]

In this work we study the co-adsorption of water with glycine, the simplest naturally occurring amino acid, using first-principles density functional theory. Although in the past some authors[32–34] have tried to account for the solvation of amino acids in the gas-phase, few studies have treated the solvation and interaction between adsorbed glycine and water molecules quantum mechanically.[35–37]

2. Method

We use CASTEP, a plane wave periodic boundary conditions DFT code,[38,39] to calculate the adsorption energy and structure of glycine co-adsorbed with water on Cu{110}. The exchange and correlation functional is that of Perdew, Burke, and Ernzerhof (PBE).[40] The calculations were performed on a Cu{110}-(3 × 2) cell for the gly and gly + H_2O phases and on a $c(2 \times 2)$ cell for pure water phases (the intact overlayer, the monomer and the half-dissociated overlayer). The Brillouin zone was sampled using a 4 × 4 × 1 Monkhorst–Pack[41] *k*-point mesh. In these calculations we employed Vanderbilt Ultrasoft Potentials[42] and the kinetic energy cut-off was fixed (as in recent calculations[43]) at 340 eV. The surface was modelled using five layers of Cu atoms, of which the bottom three layers were kept fixed. Dispersion force interactions were accounted for by using the TS pair-potential correction developed by Tkatchenko and Scheffler.[44,45] All the structures have been optimized using both PBE and PBE-TS schemes in

Department of Chemistry, University of Cambridge, Lensfield Road, Cambridge, CB2 1EW, UK. E-mail: ms857@cam.ac.uk; Fax: +44 (0)1223 762829; Tel: +44 (0)1223 763519

† Electronic supplementary information (ESI) available. See DOI: 10.1039/c3cp55094j

order to compare the effect of vdW forces on the final energies and structures using the Broyden–Fletcher–Goldfarb–Shanno (BFGS) algorithm[46] of CASTEP. In our calculations the electronic energy tolerance was 10^{-6} eV. In the geometry optimizations the force tolerance was set at 0.05 eV $Å^{-1}$.

3. Results and discussion

Glycine adsorption on Cu{110} has been previously investigated by several experimental techniques (LEED, RAIRS, STM, PhD, NEXAFS, XPS).[1,6,7,15,16,23] Early theoretical studies by this group[47] and by Sholl and co-workers[14,19,20,22] have helped establishing the three-point binding (μ_3) configuration of gly as well as the hetero-chiral footprint configuration of the (3 × 2) domains. A more recent LEED-IV structural analysis[12] of the glycine (3 × 2) overlayer on Cu{110}, which reports systematic absences in the diffraction pattern, confirms the presence of a glide-line in the adsorbates unit cell. The nominal saturation coverage of glycine on Cu{110} is two molecules adsorbed for every 6 top-layer atoms, equivalent to 1/3 ML. In the current study, we focus on gly adsorbed in a μ_3 configuration and study the influence of water on the stability of the monolayer by adding up to three H_2O monomers to the original (3 × 2) cell (Fig. 1). For a Cu{110}-(3 × 2) cell there are a total of six atop sites that can be occupied by either 2 gly molecules (the intact gly monolayer) or by 6 water molecules, hence, the mixed-phase overlayers (gly + H_2O and gly + $2H_2O$) can be constructed in three different ways by arranging a single water molecule on one of the three unoccupied copper atoms or two water molecules in three possible combinations (see ESI†). In Fig. 1 we summarize the results of the most stable among the different configurations explored.

The bonding between the glycine monomer and the surface is slightly affected by the presence of co-adsorbed water and the formation of intermolecular hydrogen bonds (Fig. 1a and e–g). Interestingly, the Cu–N bond length remains relatively constant upon hydration (d_{Cu-N} = 2.07 ± 0.04 Å), while the Cu–O bond lengths (for the oxygen atoms belonging to the carboxylate group of gly) increase up to 10% when 3 water molecules are

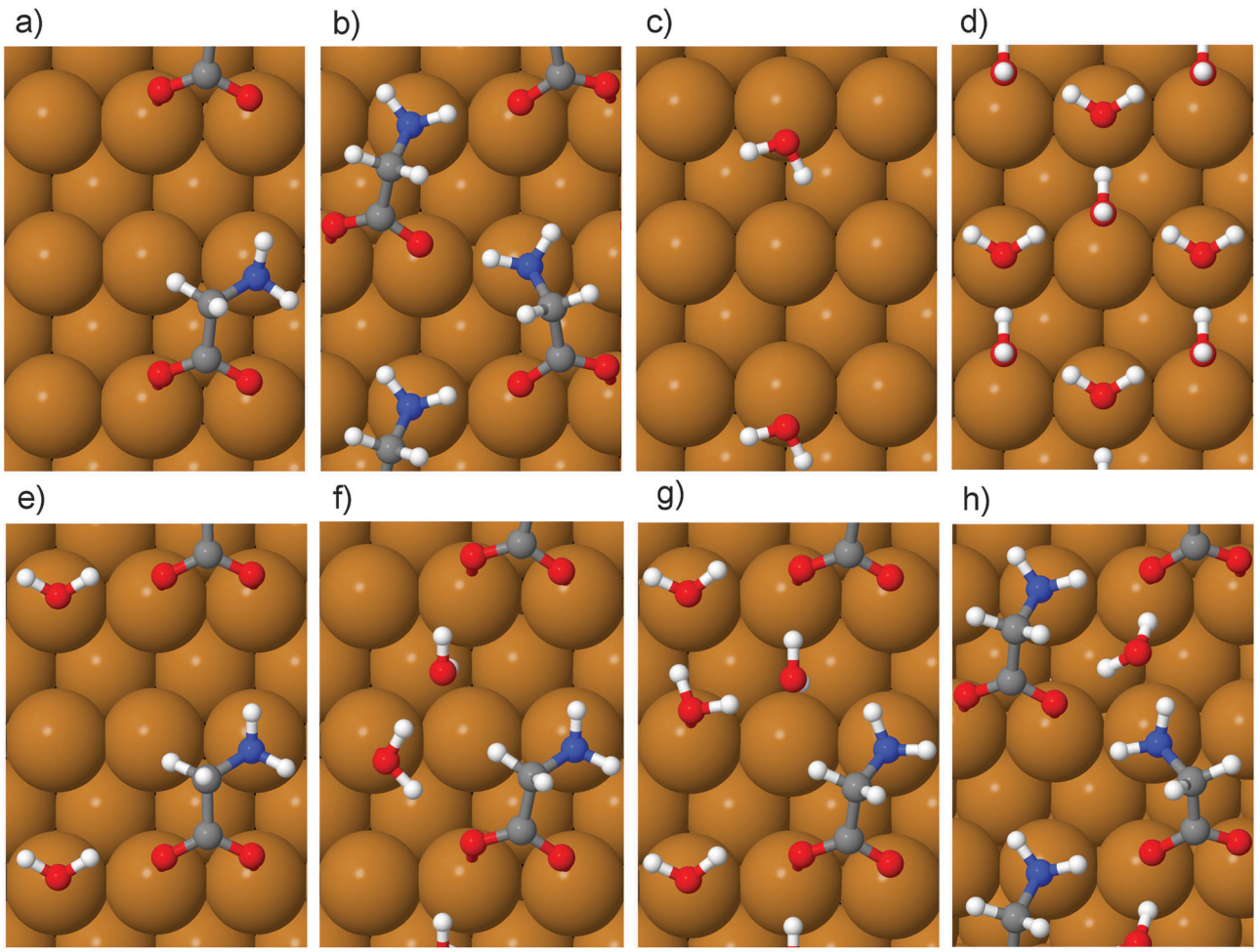

Fig. 1 Preferred glycine and water structures on Cu{110}. (a) The single glycine monomer (gly); (b) the glycine monolayer (2gly); (c) the water monomer (H_2O); (d) the water monolayer ($6H_2O$); (e) mono-hydrated glycine (gly + H_2O); (f) bi-hydrated glycine (gly + $2H_2O$); (g) tri-hydrated glycine (gly + $3H_2O$); (h) glycine monolayer mono-hydrated (2gly + H_2O).

added to the (3 × 2) cell (Fig. 1g). The addition of a single molecule of water on the saturated gly monolayer (Fig. 1h) does not significantly affect the gly–surface bonding. The bonding in the water monolayer is very similar to that reported by Jones and Jenkins,[43] with a Cu–O distance of 2.37 Å and 3.28 Å for the two water molecules in the $c(2 \times 2)$ cell (the very small difference in bond lengths between this study and the previously reported work[43] is probably due to the incorporation of vdW corrections in the present work).

The relative contribution of dispersion (van der Waals) forces and hydrogen bonding to the surface energy can be estimated by comparing the surface energy change upon H_2O addition in calculations performed with and without the TS correction. This method has been recently tested for addressing the relative intensity of hydrogen and halogen bonding compared to long-range van der Waals (vdW) interactions in phenazine overlayers and halogen-bonded supramolecular networks on graphite where it appears to perform very well.[48,49]

As mentioned in the Method section, we use a Cu{110}-(3 × 2) cell for all the calculations regarding pure gly and gly/H_2O co-adsorption, and a smaller $c(2 \times 2)$ cell to calculate the adsorption energy and surface energy for the water monomer and for the saturated (intact and half dissociated) water monolayer on Cu{110}.[50–52] The choice of a different surface cell is due to the fact that it is generally accepted that water can form pseudo-hexagonal domains on a Cu{110} surface, in which two H_2O molecules occupy non-equivalent sites on a $c(2 \times 2)$ cell.[43] Although water exhibits a surprising variety of phases[53–55] on the copper and other metal surfaces, the $c(2 \times 2)$ intact water phase is possibly the simplest phase that one can choose as a reference for the pure water layer on Cu{110}.[43]

It is well known that glycine undergoes facile dehydrogenation upon adsorption on the copper surface, so the adsorption energies we calculate are relative to the adsorbed glycine anion (glycinate). Since glycine in the gas-phase is neutral, we calculate the total adsorption energy per cell of the glycinate–water system as

$$E_{\mathrm{ads}} = \left(E_{x(\mathrm{glycinate})+y(\mathrm{H_2O})} - xE_{\mathrm{gly}} - yE_{\mathrm{H_2O}} + \frac{x}{2}E_{\mathrm{H_2}}\right), \qquad (1)$$

where $E_{x(\mathrm{glycinate})+y(\mathrm{H_2O})}$ is the energy of the adsorbed glycinate and water system per unit cell, $E_{\mathrm{H_2}}$ is the energy of the gas-phase H_2, E_{gly} and $E_{\mathrm{H_2O}}$ are the energies of the isolated (neutral) glycine and water molecule, and $E_{\mathrm{Cu\{110\}}}$ is the energy of the clean relaxed Cu{110}-(3 × 2) (or Cu{110}-$c(2 \times 2)$ for the pure adsorbed water systems) surface cell. This is equivalent to considering the product of the glycine adsorption as constituted by the adsorbed glycinate (anion) and by half a molecule of H_2 desorbed and far (non-interacting) from the surface. An alternative thermodynamic reference for the gas-phase molecule would involve calculating the total energy of the isolated glycinate, but in periodic-boundary-condition DFT calculations the energy of ionic species is normally much more difficult to calculate accurately than that of neutral species since they require calculation of the Madelung correction for the system.[56] Furthermore, it is well known experimentally that anionic glycine is not stable in the gas-phase[57,58] and, most likely, it does not desorb intact from Cu{110}, but rather dissociates on the surface at temperatures above 450–500 K.[1,3] Finally, it is worth pointing out that the long debate in the literature on the nature of the "pure" water monolayer on Cu{110} hints at the fact that water may be present on the surface in a partially-dissociated overlayer, in which some fraction of the water molecules on the surface are essentially in the anionic (hydroxyl) form OH.[43,59] The structure of the partially-dissociated overlayer has been the subject of a considerable amount of computational exploration[43,53,54,60–63] and it seems that some amount of hydroxyl (able to create stabilizing Bjerrum defects[53]) can be present in most ice structures. We have considered both the "intact" water monolayer and the "half-dissociated" water monolayer[43] by simply assuming that for each adsorbed hydroxyl mole present on the surface, half a mole of H_2 will desorb from the surface, therefore $\frac{1}{2}E_{\mathrm{H_2}}$ must be added to the above expression of E_{ads}. We also note that the quantum-nature of the proton in the H_2O networks cannot be captured by "standard" DFT calculations that treat the ionic nuclei within the boundaries of the Born–Oppenheimer approximation. Although recently reported *ab initio* path-integral molecular dynamics (PIMD) calculations for water adsorbed on Pt{111}, Ru{0001} and Ni{111} have provided valid theoretical evidence on the delocalized nature of the proton,[61] this computational method is still far too expensive to be applied on larger and more complex systems as those we have investigated here.

The adsorption energies are therefore calculated with DFT, with and without dispersion force corrections, and are reported in Table 1. The long-distance dispersion interaction between the metal surface and the adsorbed glycinate ("gly" in Table 1) is responsible for the 84% increase in the adsorption energy of the glycinate monomer in the DFT + D calculations. As one would expect, the adsorption energy per water molecule increases by only about 0.2 eV in the DFT + D results compared with the 0.7 eV increase for the gly monomer. The different increase in the adsorption energy between the two molecules can be explained by the fact that the polarizability of the small water molecule is much lower than that of the glycinate anion.

The comparison between the adsorption energies with and without vdW corrections also helps us to address the relative

Table 1 Adsorption energies, with (DFT + D) and without (DFT) vdW corrections (eV). $N_{(\mathrm{H\text{-}bonds})}$ and $E_{(\mathrm{H\text{-}bonds})}$ indicate the number of hydrogen bonds per (3 × 2) cell and the estimated total energy of the bonds[43,47]

Configuration	ΔE_{ads} (DFT)	ΔE_{ads} (DFT + D)	$N_{(\mathrm{H\text{-}bonds})}$	$E_{(\mathrm{H\text{-}bonds})}$
gly	−0.86	−1.58	0	0.00
gly + H_2O	−1.53	−2.54	2	−0.70
gly + $2H_2O$	−1.89	−3.17	4	−1.27
gly + $3H_2O$	−2.23	−4.07	7	−2.53
$6H_2O$	−0.96	−1.37	9	−5.44
2gly	−2.07	−3.70	3	−1.06
$3H_2O$	−0.30	−0.55	0	0.00
$3H_2O$ + 3OH	−0.77	−1.21	9	−4.85
2gly + H_2O	−2.18	−4.07	5	−2.09

importance of oriented H-bonds and long-range dispersion forces in the intermolecular bonding of supramolecular networks of amino acids. In fact, by simply subtracting the adsorption energy of the monomer from the adsorption energy of the dense gly network (2gly), we obtain the energy stabilization due to H-bonds formation (for the DFT results) or due to the combination of H-bonding and vdW forces (for the DFT + D results). The H-bonding accounts for 0.35 eV (65%) of the energy decrease per molecule upon network formation, while vdW forces are responsible for the remaining 0.19 eV.

Table 1 reports the number of intermolecular hydrogen bonds in a (3×2) unit cell with an estimate of the total energy of the hydrogen bonds per cell calculated using eqn (4) in ref. 43 (the hydrogen bonds lengths are reported in Fig. S3 of the ESI†). By increasing the hydration of the gly monomer the number of intermolecular hydrogen bonds increases from 2 (gly + H_2O) to 7 (gly + $3H_2O$) per surface unit cell.

The choice of a different unit cell for a water monolayer does not prevent us from comparing the relative stability of the two systems, since we can convert an extensive thermodynamic property (such as the free energy of the system) into a specific surface free energy (Γ), a property independent of the size of the surface cell.[64] The surface free energy can be obtained by subtracting from the total energy of the system the chemical potential of each species, and normalizing using the number of surface atoms:

$$\Gamma = \frac{\left(E_{x(\text{glycinate})+y(H_2O)} - x\mu_{\text{gly}} - y\mu_{H_2O} + \frac{x}{2}\mu_{H_2}\right)}{n_{\text{Cu}}} \qquad (2)$$

At 0 K and zero pressure, the gas-phase chemical potentials of H_2O and neutral glycine are simply given by the total ground state energy calculated by DFT. The chemical potential of glycinate is then obtained by subtracting the proton chemical potential $\left(\mu_H = \frac{1}{2}\mu_{H_2}\right)$ from the glycine chemical potential instead of attempting to calculate directly the energy of the ionic molecule in an isolated cell. Clearly, here we are assuming that the system (surface species and gas-phase molecules) is in perfect equilibrium, so that we can use gas-phase chemical potentials in eqn (2). The chemical potentials can be calculated as a function of temperature and pressure using standard thermodynamic equations (as described by Anghel *et al.*[64]):

$$\mu_X(T, p^0) = H_X^0(T, p^0) - TS_X(T, p^0) \qquad (3)$$

$$\mu_X(T, p) = \mu_X(T, p^0) + kT \ln(p/p^0) \qquad (4)$$

In this work we have neglected zero point energy and surface entropic contributions to the free energy of the adsorbed systems. Only low-frequency modes (and in particular frustrated translations) are likely to significantly contribute to the vibrational entropic term (at least at experimentally relevant temperatures <600 K). Unfortunately, it is very difficult to precisely calculate the vibrational mode frequencies for adsorbates on metal surfaces with periodic-boundary conditions DFT, since it would require extremely well converged forces for extensive systems (containing several tens of metal atoms). Reducing the force tolerance by almost an order of magnitude would, in our case, increase prohibitively the cost of the calculations. Furthermore, there are often significant numerical errors in the calculated normal mode frequencies for the lowest lying vibrations (frustrated translations and rotations). Although we neglected these vibrational effects, other entropic effects are accounted for in the calculation of the free energy of the system through the gas-phase ideal value of molar entropy (see eqn (3)). Similar considerations apply for the calculation of zero point energy (ZPE) contributions to the energetics, since an accurate estimate of the ZPE correction to the molar enthalpy would require the precise knowledge of the vibrational frequencies of all the phases investigated. Furthermore, with regard to the relative extent of the ZPE contribution, one can demonstrate relatively straightforwardly (see ESI†), that ZPE should not affect significantly the present results.

The results of the surface energy calculations are summarized in Table 1 and Fig. 2. Fig. 2 summarizes the results of the DFT calculations with and without vdW corrections to the intermolecular and adsorption binding energy. Under typical UHV conditions (pressure of gly and H_2 equal to 10^{-13} bar), by adding a very low amount of H_2O ($P(H_2O) = 10^{-10}$ bar) the most stable phase among those examined remains the glycine monolayer. Interestingly, it appears that the gly monolayer is stable up to a temperature of about 590 K (Fig. 2c). Shavorskiy and coauthors reported that glycinate on Cu{110} is stable up to 480 K; above this temperature glycine begins to dissociate on the surface, therefore their results suggest that the molecule–surface bonds are stronger than the glycinate intramolecular bonds, reinforcing the agreement between the theoretically predicted stability of gly and the experimental observations.[1] The predicted hydrogen bond energy per cell in the water monolayer (Table 1) could potentially be much higher than in the glycine and mixed gly–water phases, it is therefore clear that the relative stability of the different phases can be rationalized only by considering that the energy calculated by DFT accounts for electrostatic and dipole–dipole repulsive effects that destabilize the water monolayers.

LEED and RAIRS results,[65] as well as previous DFT calculations[22] show that gly forms stable, ordered monolayers in which every molecule assumes a tridentate binding configuration; therefore in the present study we have not investigated the relative stability of other (bidentate) binding configurations. By incorporating vdW corrections in the DFT calculations (Fig. 2c) the range of stability of the gly monolayer increases up to about 590 K. It is well known that semiempirical vdW corrections generally overestimate the absolute adsorption energies on metals, therefore it is not surprising that we obtained a rather wider range of stability for gly on Cu{110} than what is experimentally reported. If we now focus on the effects of the water pressure on the surface co-adsorption equilibrium with gly, we can see (Fig. 2b) that increasing the water pressure to 10^{-5} bar can cause water (in its half-dissociated form H_2O + OH) to completely displace gly from the Cu{110} surface. Finally, for the vdW corrected calculations,

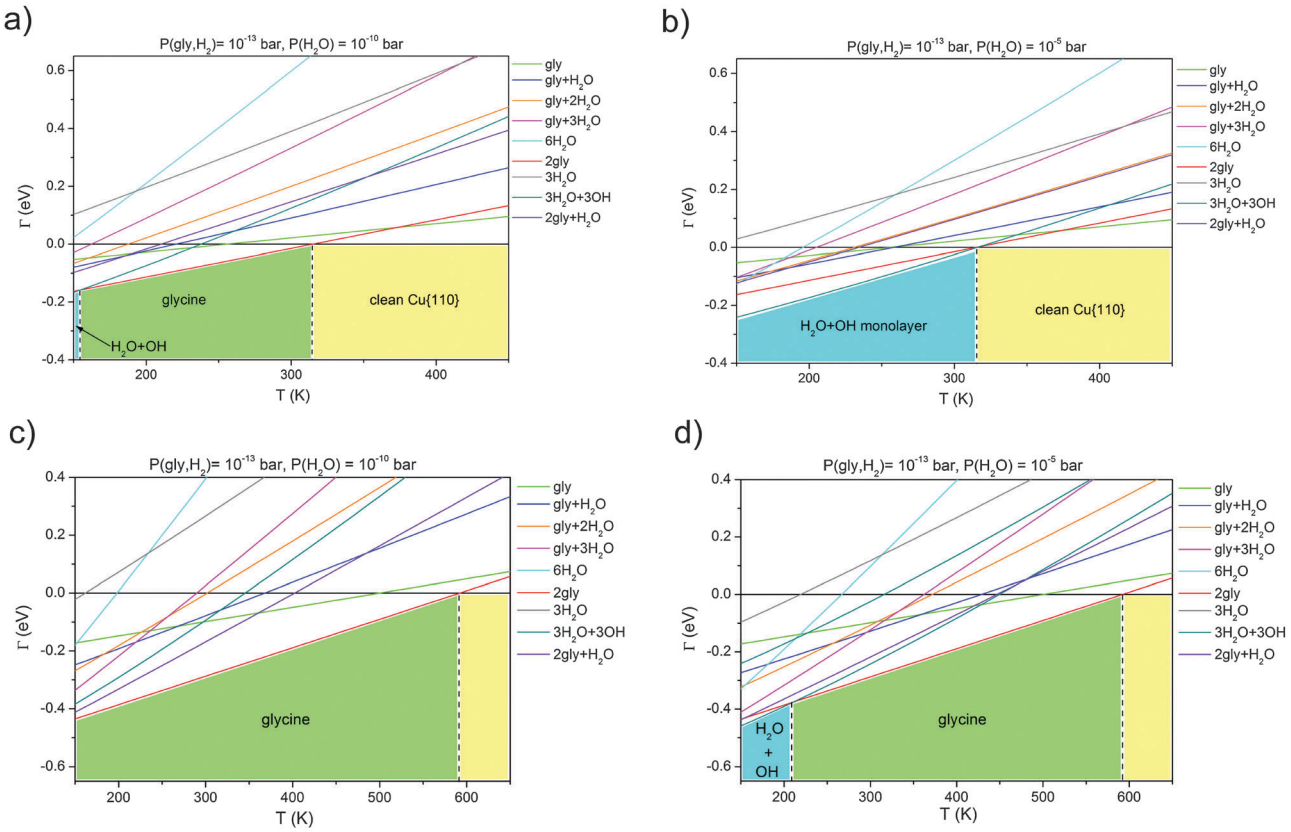

Fig. 2 Phase diagrams at constant pressure for glycine and water on Cu{110} calculated without (a and b) and with (c and d) dispersion force (vdW) corrections. The solid lines indicate the surface energy Γ (eV) as a function of the temperature T (K) for several different glycine and water phases on Cu{110}. The green region highlights the range of stability for the gly monolayer while the cyan region indicates the temperature range in which the half dissociated (H_2O + OH) water overlayer is the most stable. The yellow region indicates the region in which no overlayer is stable on the Cu{110} surface.

we can see that by increasing the water pressure to 10^{-5} bar (Fig. 2d), the half-dissociated water monolayer is the most stable phase for a low surface temperature ($T < \sim 200$ K), but that the gly monolayer is still stable from medium to high temperature. The results are summarized in a complete phase diagram of gly and H_2O on Cu{110} with (Fig. 3) and without (Fig. 4) vdW corrections in the calculations of the surface energies for the different gly and H_2O co-adsorbed systems.

The recent results reported by Shavorskiy *et al.*[1] seem to suggest that glycine and water phases can mix and that chemical reactions (for water pressure above 10^{-5} mbar) between co-adsorbed species occur at around room temperature. Since the vast majority of surface reactions follow a Langmuir–Hinshelwood mechanism[66] (whose first requirement is that all the reactants will be sitting on adjacent neighbouring sites) it would seem more intuitive that a phase separation between adsorbed water (forming a so-called two-dimensional ''ice'' overlayer) and glycine would not allow the quick reaction steps proposed by Shavorskiy and co-authors. Surprisingly then, our results show that, over a wide range of temperature and pressure, the pure water and glycine overlayers are more stable than the mixed phases, suggesting that the ability to form intermixed hydrogen-bonded networks between the anionic amino acid and water is not the reason

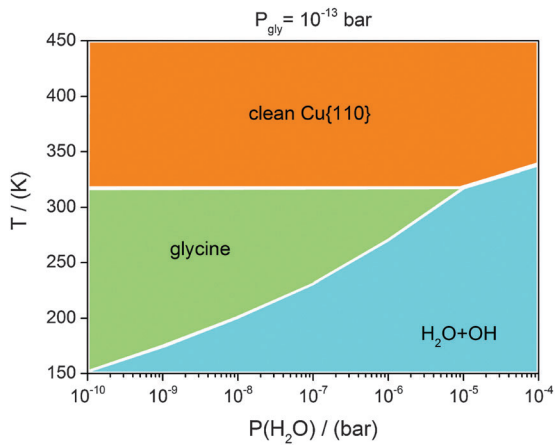

Fig. 3 The phase diagram for the glycine/H_2O equilibrium (without vdW corrections) as a function of the surface temperature (T) and water pressure $P(H_2O)$. The pressure of glycine is kept constant at 10^{-13} bar. The region of thermodynamic stability for the glycine monolayer is in green, for the half dissociated water monolayer it is in cyan and for the clean Cu{110} surface it is in orange.

behind the extraordinary reactivity between H_2O and gly (or ala). The reaction between radical and ionic species (adsorbed O for instance) with glycine could happen at the boundary

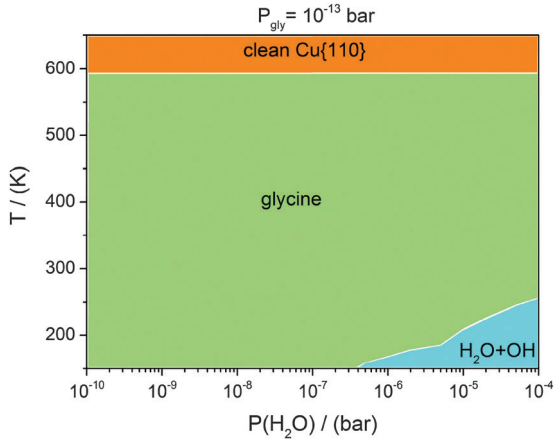

Fig. 4 The phase diagram for the glycine/H_2O equilibrium (with vdW corrections) as a function of the surface temperature (T) and water pressure $P(H_2O)$. The pressure of glycine is kept constant at 10^{-13} bar. The region of thermodynamic stability for the glycine monolayer is in green, for the half dissociated water monolayer it is in cyan and for the clean Cu{110} surface it is in orange.

regions between glycine and water islands or the amino acid dissociation could follow an Eley–Rideal mechanism, in which adsorbed glycine reacts with the incoming water vapour. If we consider that Shavorskiy *et al.*[67] found no evidence of reaction between glycine and water when the Cu{110} surface was pre-saturated by glycine, we can also exclude the fact that the reaction could proceed through an Eley–Rideal mechanism; therefore the only alternative remaining is that, at submonolayer coverage, the glycine islands are surrounded by a reactive water boundary region.

Clearly, we are not aiming within the present work to address the complexity of the microkinetic mechanism suggested in ref. 1, but our purpose here is essentially to show that DFT calculations including (at least at the semi-empirical level[44]) long-range intermolecular interactions can be an important tool in attempting to investigate both the structure and the reactivity of co-adsorbed polar and hydrogen-bonded adsorbates.

4. Conclusions

In this work we have explored the interaction and the relative thermodynamic stability of glycine and water co-adsorbed on Cu{110}. Both the strength of the adsorbate–surface binding and the intensity of the intermolecular bonding in glycine and water overlayers is significantly affected by the inclusion of dispersion interactions.[44] A thermodynamic exploration allowed us a glimpse of the complexity of the two-dimensional phase diagram of gly and water on Cu{110}. In particular, our results are consistent with recently reported reactivity studies in which the temperature range of stability for glycine and alanine on Cu{110} was significantly reduced by increasing the pressure of water.[1] We have therefore demonstrated that DFT calculations can be useful to address the thermodynamics of complex surface co-adsorbed phases relevant to surface chirality as well as to corrosion and surface-protection properties of organic molecules on metal surfaces. Further theoretical and experimental work is needed to explore the reported reactions between water and glycine at different pressure and temperature conditions, as well as to identify the nature and the strength of the intermolecular bonding between neighbouring molecules.

Acknowledgements

The authors acknowledge Prof. Georg Held for insightful discussions and comments. This work was performed using the Darwin Supercomputer of the University of Cambridge High Performance Computing Service, provided by Dell Inc. using Strategic Research Infrastructure Funding from the Higher Education Funding Council for England. This work was funded by the EPSRC grant EP/J001643/1.

References

1 A. Shavorskiy, F. Aksoy, M. E. Grass, Z. Liu, H. Bluhm and G. Held, *J. Am. Chem. Soc.*, 2011, **133**, 6659–6667.
2 M. Blanco-Rey and G. Jones, *Phys. Rev. B: Condens. Matter Mater. Phys.*, 2010, **81 x**, 205428.
3 S. M. Barlow, S. Louafi, R. D. Le, J. Williams, C. Muryn, S. Haq and R. Raval, *Surf. Sci.*, 2005, **590**, 243–263.
4 S. M. Barlow, S. Louafi, D. Le Roux, J. Williams, C. Muryn, S. Haq and R. Raval, *Langmuir*, 2004, **20**, 7171–7176.
5 M. Nyberg, M. Odelius, A. Nilsson and L. G. M. Pettersson, *J. Chem. Phys.*, 2003, **119**, 12577–12585.
6 N. A. Booth, D. P. Woodruff, O. Schaff, T. Gießel, R. Lindsay, P. Baumgärtel and A. M. Bradshaw, *Surf. Sci.*, 1998, **397**, 258–269.
7 S. M. Barlow, K. J. Kitching, S. Haq and N. V. Richardson, *Surf. Sci.*, 1998, **401**, 322–335.
8 M. Forster, M. Dyer, M. Persson and R. Raval, *Top. Catal.*, 2011, **54**, 13–19.
9 M. Forster, M. S. Dyer, M. Persson and R. Raval, *Angew. Chem., Int. Ed.*, 2010, **49**, 2344–2348.
10 M. Forster, M. S. Dyer, M. Persson and R. Raval, *J. Am. Chem. Soc.*, 2009, **131**, 10173–10181.
11 E. Mateo Marti, S. M. Barlow, S. Haq and R. Raval, *Surf. Sci.*, 2002, **501**, 191–202.
12 Z. V. Zheleva, T. Eralp and G. Held, *J. Phys. Chem. C*, 2011, **116**, 618–625.
13 R. B. Rankin and D. S. Sholl, *J. Chem. Phys.*, 2006, **124**, 074703.
14 R. B. Rankin and D. S. Sholl, *J. Phys. Chem. B*, 2005, **109**, 16764–16773.
15 J. H. Kang, R. L. Toomes, M. Polcik, M. Kittel, J. T. Hoeft, V. Efstathiou, D. P. Woodruff and A. M. Bradshaw, *J. Chem. Phys.*, 2003, **118**, 6059–6071.
16 R. L. Toomes, J. H. Kang, D. P. Woodruff, M. Polcik, M. Kittel and J. T. Hoeft, *Surf. Sci.*, 2003, **522**, L9–L14.

17 V. Efstathiou and D. P. Woodruff, *Surf. Sci.*, 2003, **531**, 304–318.
18 N. Lorente, M. F. G. Hedouin, R. E. Palmer and M. Persson, *Phys. Rev. B: Condens. Matter Mater. Phys.*, 2003, **68**, 155401.
19 J. W. Han, J. N. James and D. S. Sholl, *J. Chem. Phys.*, 2011, **135**, 034703.
20 J. N. James and D. S. Sholl, *J. Mol. Catal. A: Chem.*, 2008, **281**, 44–48.
21 S. Blankenburg and W. G. Schmidt, *Nanotechnology*, 2007, **18**, 424030.
22 R. B. Rankin and D. S. Sholl, *Surf. Sci.*, 2004, **548**, 301–308.
23 Q. Chen, D. J. Frankel and N. V. Richardson, *Surf. Sci.*, 2002, **497**, 37–46.
24 J. Hasselström, O. Karis, M. Weinelt, N. Wassdahl, A. Nilsson, M. Nyberg, L. G. M. Pettersson, M. G. Samant and J. Stöhr, *Surf. Sci.*, 1998, **407**, 221–236.
25 D. A. Duncan, M. K. Bradley, W. Unterberger, D. Kreikemeyer-Lorenzo, T. J. Lerotholi, J. Robinson and D. P. Woodruff, *J. Phys. Chem. C*, 2012, **116**, 9985–9995.
26 K. Kanazawa, A. Taninaka, H. Huang, M. Nishimura, S. Yoshida, O. Takeuchi and H. Shigekawa, *Chem. Commun.*, 2011, **47**, 11312–11314.
27 X. Zhao, H. Yan, R. G. Zhao and W. S. Yang, *Langmuir*, 2002, **19**, 809–813.
28 L. L. Atanasoska, J. C. Buchholz and G. A. Somorjai, *Surf. Sci.*, 1978, **72**, 189–207.
29 Y. Kim, *J. Korean Chem. Soc.*, 2010, **54**, 680–686.
30 K. F. Khaled, *Corros. Sci.*, 2010, **52**, 3225–3234.
31 D.-Q. Zhang, Q.-R. Cai, X.-M. He, L.-X. Gao and G.-D. Zhou, *Mater. Chem. Phys.*, 2008, **112**, 353–358.
32 A. D. Kulkarni, D. Rai, S. P. Gejji, L. J. Bartolotti and R. K. Pathak, *Int. J. Quantum Chem.*, 2013, **113**, 1325–1332.
33 B. Balta and V. Aviyente, *J. Comput. Chem.*, 2003, **24**, 1789–1802.
34 S. M. Bachrach, *J. Phys. Chem. A*, 2008, **112**, 3722–3730.
35 D. Costa, A. Tougerti, F. Tielens, C. Gervais, L. Stievano and J. F. Lambert, *Phys. Chem. Chem. Phys.*, 2008, **10**, 6360–6368.
36 E. Jimenez-Izal, F. Chiatti, M. Corno, A. Rimola and P. Ugliengo, *J. Phys. Chem. C*, 2012, **116**, 14561–14567.
37 A. Rimola, M. Corno, C. M. Zicovich-Wilson and P. Ugliengo, *Phys. Chem. Chem. Phys.*, 2009, **11**, 9005–9007.
38 S. J. Clark, M. D. Segall, C. J. Pickard, P. J. Hasnip, M. J. Probert, K. Refson and M. C. Payne, *Z. Kristallogr.*, 2005, **220**, 567–570.
39 M. D. Segall, P. J. D. Lindan, M. J. Probert, C. J. Pickard, P. J. Hasnip, S. J. Clark and M. C. Payne, *J. Phys.: Condens. Matter*, 2002, **14**, 2717–2744.
40 J. P. Perdew and Y. Wang, *Phys. Rev. B: Condens. Matter Mater. Phys.*, 1992, **45**, 13244.
41 H. J. Monkhorst and J. D. Pack, *Phys. Rev. B: Condens. Matter Mater. Phys.*, 1976, **13**, 5188.
42 D. Vanderbilt, *Phys. Rev. B: Condens. Matter Mater. Phys.*, 1990, **41**, 7892.
43 G. Jones and S. J. Jenkins, *Phys. Chem. Chem. Phys.*, 2013, **15**, 4785–4798.
44 A. Tkatchenko and M. Scheffler, *Phys. Rev. Lett.*, 2009, **102**, 073005.
45 E. R. McNellis, J. Meyer and K. Reuter, *Phys. Rev. B: Condens. Matter Mater. Phys.*, 2009, **80**, 205414.
46 B. G. Pfrommer, M. Côté, S. G. Louie and M. L. Cohen, *J. Comput. Phys.*, 1997, **131**, 233–240.
47 G. Jones, S. J. Jenkins and D. A. King, *Surf. Sci.*, 2006, **600**, L224–L228.
48 A. Y. Brewer, M. Sacchi, J. E. Parker, C. L. Truscott, S. J. Jenkins and S. M. Clarke, *Mol. Phys.*, 2013, 1–8.
49 M. Sacchi, A. Y. Brewer, S. J. Jenkins, J. E. Parker, T. Friščić and S. M. Clarke, *Langmuir*, 2013, **29**, 14903.
50 J. Lee, D. C. Sorescu, K. D. Jordan and J. T. Yates, *J. Phys. Chem. C*, 2008, **112**, 17672–17677.
51 T. Schiros, H. Ogasawara, L. A. Naslund, K. J. Andersson, J. Ren, S. Meng, G. S. Karlberg, M. Odelius, A. Nilsson and L. G. M. Pettersson, *J. Phys. Chem. C*, 2010, **114**, 10240–10248.
52 T. Schiros, S. Haq, H. Ogasawara, O. Takahashi, H. Öström, K. Andersson, L. G. M. Pettersson, A. Hodgson and A. Nilsson, *Chem. Phys. Lett.*, 2006, **429**, 415–419.
53 M. Forster, R. Raval, A. Hodgson, J. Carrasco and A. Michaelides, *Phys. Rev. Lett.*, 2011, **106**, 046103.
54 J. Carrasco, A. Michaelides, M. Forster, S. Haq, R. Raval and A. Hodgson, *Nat. Mater.*, 2009, **8**, 427–431.
55 C. Ammon, A. Bayer, H. P. Steinruck and G. Held, *Chem. Phys. Lett.*, 2003, **377**, 163–169.
56 G. Makov and M. C. Payne, *Phys. Rev. B: Condens. Matter Mater. Phys.*, 1995, **51**, 4014.
57 R. M. Balabin, *Phys. Chem. Chem. Phys.*, 2012, **14**, 99–103.
58 B. Brauer, G. M. Chaban and R. B. Gerber, *Phys. Chem. Chem. Phys.*, 2004, **6**, 2543–2556.
59 T. Kumagai, M. Kaizu, H. Okuyama, S. Hatta, T. Aruga, I. Hamada and Y. Morikawa, *Phys. Rev. B: Condens. Matter Mater. Phys.*, 2010, **81**, 045402.
60 J. Carrasco, B. Santra, J. Klimeš and A. Michaelides, *Phys. Rev. Lett.*, 2011, **106**, 026101.
61 X. Z. Li, M. I. J. Probert, A. Alavi and A. Michaelides, *Phys. Rev. Lett.*, 2010, **104**, 066102.
62 A. Michaelides and K. Morgenstern, *Nat. Mater.*, 2007, **6**, 597–601.
63 P. J. Feibelman, *Nat. Mater.*, 2009, **8**, 372–373.
64 A. T. Anghel, S. J. Jenkins, D. J. Wales and D. A. King, *J. Phys. Chem. B*, 2006, **110**, 4147–4156.
65 S. M. Barlow and R. Raval, *Surf. Sci. Rep.*, 2003, **50**, 201–341.
66 R. J. Baxter and P. Hu, *J. Chem. Phys.*, 2002, **116**, 4379–4381.
67 A. Shavorskiy, T. Eralp, K. Schulte, H. Bluhm and G. Held, *Surf. Sci.*, 2013, **607**, 10–19.